



Title	An aptamer ligand based liposomal nanocarrier system that targets tumor endothelial cells
Author(s)	Ara, Mst Naznin; Matsuda, Takashi; Hyodo, Mamoru; Sakurai, Yu; Hatakeyama, Hiroto; Ohga, Noritaka; Hida, Kyoko; Harashima, Hideyoshi
Citation	Biomaterials, 35(25), 7110-7120 <a href="https://doi.org/10.1016/j.biomaterials.2014.04.087">https://doi.org/10.1016/j.biomaterials.2014.04.087</a>
Issue Date	2014-08
Doc URL	<a href="http://hdl.handle.net/2115/57445">http://hdl.handle.net/2115/57445</a>
Type	article (author version)
File Information	WoS_66920_Sakurai.pdf



[Instructions for use](#)

1 **An aptamer ligand based liposomal nanocarrier system that targets tumor endothelial**  
2 **cells**

3

4 **Mst. Naznin Ara<sup>a,†</sup>, Takashi Matsuda<sup>b,†</sup>, Mamoru Hyodo<sup>a</sup>, Yu Sakurai<sup>a</sup>, Hiroto**  
5 **Hatakeyama<sup>a</sup>, Noritaka Ohga<sup>c</sup>, Kyoko Hida<sup>c</sup>, Hideyoshi Harashima<sup>a,b,\*</sup>**

6 <sup>a</sup>Laboratory of Innovative Nanomedicine, Faculty of Pharmaceutical Sciences, Hokkaido  
7 University, Kita 12, Nishi 6, Kita-ku, Sapporo, Hokkaido 060-0812, Japan. <sup>b</sup>Laboratory for  
8 Molecular Design of Pharmaceutics, Faculty of Pharmaceutical Sciences, Hokkaido  
9 University, Kita 12, Nishi 6, Kita-ku, Sapporo, Hokkaido 060-0812, Japan. <sup>c</sup>Division of  
10 Vascular Biology, Graduate School of Dental Medicine, Hokkaido University, Kita 13, Nishi  
11 7, Kita-ku, Sapporo, Hokkaido 060-0812, Japan.

12

13

14

15

16 <sup>†</sup> Those authors were equally contributed.

17 \* To whom correspondence may be addressed

18 Professor Hideyoshi Harashima, Ph. D

19 Faculty of Pharmaceutical Sciences, Hokkaido University

20 Kita-12, Nishi-6, Kita-ku, Sapporo, Hokkaido 060-0812, Japan.

21 Tel.: +81 11 706 2197; fax: +81 11 706 4879.

22 E-mail: [harasima@pharm.hokudai.ac.jp](mailto:harasima@pharm.hokudai.ac.jp)

23 ABSTRACT

24 The objective of this study was to construct our recently developed aptamer-modified  
25 targeted liposome nano-carrier (Apt-PEG-LPs) system to target primary cultured mouse  
26 tumor endothelial cells (mTEC), both *in vitro* and *in vivo*. We first synthesized an aptamer-  
27 polyethylene glycol 2000-distearoyl phosphoethanolamine (Apt-PEG<sub>2000</sub>-DSPE). The  
28 conjugation of the Apt-PEG<sub>2000</sub>-DSPE was confirmed by MALDI-TOF mass spectroscopy. A  
29 lipid hydration method was used to prepare Apt-PEG-LPs, in which the the outer surface of  
30 the PEG-spacer was decorated with the aptamer. Apt-PEG-LPs were significantly taken up  
31 by mTECs. Cellular uptake capacity was observed both quantitatively and qualitatively using  
32 spectrofluorometry, and confocal laser scanning microscopy (CLSM), respectively. In  
33 examining the extent of localization of aptamer-modified liposomes that entered the cells,  
34 approximately 39% of the Apt-PEG-LPs were not co-localized with lysotracker, indicating  
35 that they had escaped from endosomes. The uptake route involved a receptor mediated  
36 pathway, followed by clathrin mediated endocytosis. This Apt-PEG-LP was also applied for  
37 *in vivo* research whether this system could target tumor endothelial cells. Apt-PEG-LP and  
38 PEG<sub>5000</sub>-DSPE modified Apt-PEG-LP (Apt/PEG<sub>5000</sub>-LP) were investigated by human renal  
39 cell carcinoma (OS-RC-2 cells) inoculating mice using CLSM. Apt-PEG-LP and  
40 Apt/PEG<sub>5000</sub>-LP showed higher accumulation on tumor vasculature compared to PEG-LP and  
41 the co-localization efficacy of Apt-PEG-LP and Apt/PEG<sub>5000</sub>-LP on TEC were quantified  
42 16% and 25% respectively, which was also better than PEG-LP (3%). The findings suggest  
43 that this system is considerable promise for targeting tumor endothelial cells to deliver drugs  
44 or genes *in vitro* and *in vivo*.

45

46 **Key words:** Targeted delivery, Aptamer-liposomes, Endocytosis, Intracellular uptake

47

48

49 *Abbreviations:* LPs, Liposomes; Apt, Aptamer; PEG, maleimide-PEG<sub>2000</sub>-DSPE; PEG-LPs,  
50 maleimide-PEG<sub>2000</sub>-DSPE modified liposomes; Apt-PEG-LPs, Aptamer modified maleimide-  
51 PEG<sub>2000</sub>-DSPE liposomes; mTECs: Primary cultured mouse tumor endothelial cells

52

53

## 54 **1. Introduction**

55 A continuous affordable, but still greater challenge remains in nano-medicine in terms of  
56 cancer diagnosis, and therapy designed to deliver imaging agents or chemotherapeutic drugs  
57 to cells in a specific and selective manner [1]. The successful delivery of cytotoxic drugs via  
58 passive or active targeting is an important issue in the design and construction of new and  
59 improved targeting drug delivery systems. Small molecules such as peptides, as well as  
60 antibodies have been widely used targeting agents, and has enjoyed some (but not sufficient)  
61 success, when incorporated with nano-materials. The resulting constructs are often dictated  
62 more by the materials used rather than the targeting agents. Researchers are currently  
63 attempting to develop more and more new types of therapy [2-5]. To meet these challenges,  
64 nucleic acid aptamers are now of great interest as new targeting small molecules. Aptamers  
65 are single stranded oligonucleotides, ssDNA or ssRNA molecules produced by SELEX [6, 7].  
66 Cell-SELEX is a modified selection method against live cells [8]. Aptamers are very easy to  
67 reproduce, are low in cost, generally nontoxic, and have a low molecular weight (8-15 kDa).  
68 This single stranded DNA or RNA oligonucleotide can fold into well-defined 3D structures  
69 and bind to their target with a high affinity ( $\mu\text{M}$  to  $\text{pM}$  range) and specificity [9, 10].

70 As a ligand, aptamers possess several advantages over other ligands that are used in drug  
71 delivery such as antibodies. First, the production of aptamers doesn't require any biological  
72 system and, hence, is much easier to scale up with low batch-to-batch variability [11]. Second,  
73 aptamers are quite thermally stable and can be denatured and renatured multiple times  
74 without any loss of activity. Third, aptamers can be chemically modified to enhance their  
75 stability in biological fluids, because of their smaller size; they are able to easily and rapidly  
76 diffuse into tissues and organs and thus permit faster targeting in drug delivery. Lastly,  
77 conjugation chemistry for attaching various imaging labels or functional groups to aptamers  
78 is orthogonal to nucleic acid chemistry, and hence they can be readily introduced during

79 aptamer synthesis. Extensive research on aptamers indicate that they have great potential for  
80 use in a variety of areas, including diagnosis, therapy, biomarker identification, and, most  
81 promising, as a targeting ligand for developing new drug delivery systems [8-12]. Macugen  
82 (Pegaptanib) is the first nucleic acid aptamer that was approved by the US Food and Drug  
83 Administration in December 2004 as an anti-angiogenic therapeutic agent for neovascular  
84 (wet) age related macular degeneration. A variety of aptamers against other molecular targets  
85 are currently undergoing clinical investigation [13, 14].

86 As of this writing, liposomes are the most successful drug delivery system available. From  
87 the first discovery to date, many liposomal formulations have been approved by the US Food  
88 and Drug Administration, and many are in preclinical and clinical trials in different fields  
89 [15-18]. This class of nano-particles improve the solubility, toxicity profile, and unfavorable  
90 pharmacokinetics of a chemotherapeutic. However, therapeutic efficacy remains a big  
91 challenge and is largely unchanged. As a result, the development of a tool to allow constant  
92 and selective delivery would be highly desirable. The key problems of drug therapy such as  
93 bio-distribution throughout the body and targeting to specific receptors could be improved by  
94 using a ligand based liposomal formulation [19]. PEGylated liposomes, also known as stealth  
95 liposome possess some advantages, including longer circulation time, and have the ability to  
96 passively accumulate in tumor tissues or organs, although, they have been reported to have  
97 insufficient cellular-uptake and endosomal escape properties, a fact that reduces the  
98 pharmacological effect of the drug, this phenomenon is commonly referred to as the PEG-  
99 dilemma. To increase the efficacy of delivery to target tissues, aptamer modified liposomes  
100 can be considered as good candidates. After Willis's pioneering work on 1998 [20], the drug  
101 delivery using aptamer modified liposomes have been investigated well [21-23]. A few in  
102 vivo research studies were also initiated and the aptamer mediated liposomal active targeting  
103 strategy appears to hold considerable promise for use as a liposomal drug delivery system [24,

104 25]. Many of the aptamer-liposome drug delivery systems have been applied to targeting  
105 cancer parenchymal cells and not the tumor vasculature. The goal of this study was to  
106 examine the the use of target-specific ligand aptamer modified liposomes, an alternative  
107 promising approach, to reduce the side effects associated with PEG and thus, allow targeting  
108 to the tumor vasculature with better efficacy [26].

109       Angiogenesis-dependant tumor growth was first reported by Folkman in 1971 [27].  
110 Preventing or inhibiting angiogenesis is associated with the increased vascularity necessary  
111 for tumor progression and metastasis. Metastases are the cause of 90% of all human cancer  
112 deaths. Chemotherapy of cancer metastases, which are effective in some patients, are often  
113 associated with significant toxicity, due to the nonspecific distribution of cytotoxic drugs  
114 which limits the maximum allowable dose [28, 29]. Tumor blood vessels provide nutrients  
115 and oxygen, and remove waste from tumor tissue, thus enhancing tumor progression. Tumor  
116 blood vessels have been shown to differ from their normal counterparts in that they show  
117 leakiness and have a basement membrane that is thick and uneven. This suggests that tumor  
118 endothelial cells may well express surface markers that are different from those found in  
119 normal cells [30, 31]. Our rationale for targeting tumor endothelial cells in our current project  
120 is based on the following assumptions, Tumor endothelial cells can support many tumor cells,  
121 and thus, targeting endothelial cells might be a much more effective strategy than targeting  
122 actual tumor cells themselves. In fact, active targeting can be achieved by the efficient  
123 recognition of specific antigens that are expressed on the cell surface proteins of tumor cells  
124 but are not expressed on normal cells [32-36]. Therefore, the ligand attached on the surface of  
125 PEGylated liposomes such as Apt-PEG-LPs can be enhanced the cellular uptake.

126       We recently isolated a DNA aptamer AraHH001 ( $K_d = 43$  nM) that is selectively  
127 expressed on the mates of different origin and does not bind to healthy endothelial cells.  
128 Additionally, this aptamer has a high internalization capacity [37], providing a means for the

129 intracellular delivery of drugs or gene therapy that are themselves not permeable to cells. For  
130 this reason, we selected this high affinity aptamer for use in the current study. We established  
131 a aptamer-based mTECs targeted liposomal drug delivery system which enhanced the uptake  
132 into target mTECs compared to PEGylated liposomes, and conducted a detailed study of the  
133 uptake mechanism and intracellular trafficking for this system.

134

## 135 **2. Methods**

### 136 *2.1. Synthesis of a DNA aptamer AraHH001 conjugated Maleimide-PEG<sub>2000</sub>-DSPE.*

137 The conjugation of the AraHH001 aptamer  
138 (ACGTACCGACTTCGTATGCCAACAGCCCTTTATCCACCTC) (100 nmol) reacted with  
139 a 5 times excess of Maleimide-PEG<sub>2000</sub>-DSPE was performed by a gentle overnight soaking  
140 in a Bio-shaker at room temperature. AraHH001 was purchased from Sigma-Genosys. For  
141 the conjugation reaction, the disulphide (S-S) bonds of AraHH001 were first cleaved by  
142 treatment with an excess TCEP solution on ice for 30-40 min. After the conjugation reaction,  
143 the excess maleimide-PEG<sub>2000</sub>-DSPE was removed by dialysis (MWCO 3500-5000) in 1%  
144 SDS, 50 mM phosphate buffer at pH 7 with the solvent being changed three times at 4 h  
145 intervals. Further dialysis was performed in 50 mM ammonium hydrogen carbonate buffer at  
146 pH 8.0 by changing the solvent three times at every 4 h interval. The purified aptamer-lipid  
147 conjugation was ion-exchanged with Zip-Tip C18 and examined by agarose-gel  
148 electrophoresis and MALDI-TOF mass spectroscopy.

149

### 150 *2.2. Preparation of liposomes.*

151 Liposomes (LPs) formulations were prepared by the standard lipid hydration method. The  
152 molar ratio of EPC, Chol and Rhodamine-DOPE was 70:30:1. About 5 mole% of PEG<sub>2000</sub>-  
153 DSPE or Apt-PEG<sub>2000</sub>-DSPE of the total lipid was added to the lipid solutions during the  
154 preparation of the PEG-LPs or Apt-PEG-LPs respectively. All lipids were dissolved in  
155 chloroform/ethanol solutions, and, a lipid film was prepared by evaporating all of the solvents  
156 under a stream of nitrogen gas. The dried lipid film was hydrated by adding HEPES buffer  
157 (10 mM, pH = 7.4) for 10 min at room temperature, followed to the sonication for  
158 approximately 30sec-1 min in a bath type sonicator (AU-25 C, Aiwa, Tokyo, Japan). The  
159 average size and diameter of liposomes were measured by using a Zetasizer Nano ZS  
160 ZEN3600 (Malvern Instrument, Worcestershire, UK).

161

### 162 *2.3. Isolation of mouse tumor endothelial cells (mTECs).*

163 All experiments involving animals and their care were carried out consistent with  
164 Hokkaido University guidelines, and protocols approved by the Institutional Animal Care and  
165 Use Committee. Endothelial cells were isolated as previously described [32-36]. Briefly,  
166 normal endothelial cells NECs were isolated from the dermis as controls. TECs were isolated  
167 by magnetic bead cell sorting using an IMag cell separating system (BD Bioscience). CD31-  
168 Positive cells were sorted and plated on 1.5% gelatin-coated culture plates and grown in  
169 EGM-2 MV (Clonetics, Walkers, MD) and 15% FBS. Diphtheria toxin (DT) (500 ng/mL,  
170 Calbiochem, San Diego, CA) was added to the TEC subcultures to kill any remaining human  
171 tumor cells. Human cells express heparin-binding EGF-like growth factor (hHB-EGF), a DT-  
172 receptor. However, DT does not interact with mouse HB-EGF and murine ECs survive this  
173 treatment.

174

### 175 *2.4. Maintenance of cell cultures.*

176 Human renal cell carcinoma, OS-RC-2 cells were cultured in RPMI-1640, containing 10%  
177 fetal bovine serum, penicillin (100 U/mL) and streptomycin (100 µg/mL). Primary cultured  
178 TECs were cultured using a special medium, namely EGM-2 MV (Lonza). To prevent  
179 microbial growth, penicillin (100 unit/mL) and (100 µg/mL) streptomycin were added to the  
180 EGM-2 MV. Cell cultures were maintained at 37 °C in a 5% CO<sub>2</sub> incubator at 95% humidity.  
181 For regular cell cultures a 0.1% trypsin solution was used to dissociate the cells from the  
182 surface of the culture dish. However, during the entire selection of a DNA aptamer, flow  
183 cytometry assay and during aptamer targeted protein purification, RepCell was used (cell  
184 seed Inc., Tokyo, Japan).

185

#### 186 *2.5. Quantitative cellular uptake analysis of Apt-PEG-LPs in mTECs by spectrofluorometer.*

187 To perform a quantitative cellular uptake analysis,  $4 \times 10^4$  cells were seeded per cm<sup>2</sup> in  
188 24-well plates (Corning Incorporated, Corning, NY, USA) and incubated overnight at 37 °C  
189 in an atmosphere of 5% CO<sub>2</sub>, and in 95% humidity. On the next experimental day, medium  
190 from cells in 24 well-plates was removed by aspiration and the cells then washed with warm  
191 PBS once. A different rhodamine labeled liposomal solution was then added to the cells,  
192 followed by incubation for 3 h at 37 °C in an atmosphere of 5% CO<sub>2</sub>, and in 95% humidity.  
193 After 3 h of incubation, the cells were washed with 1× warm PBS supplemented with 100 nM  
194 cholic acid twice and the cells were then incubated with 1× Reporter lysis buffer at -80 °C to  
195 lysis and after 20 min, they were put on ice to melt treated cell suspensions were treated with  
196 the different liposome solution in 24-well plates. Finally, the lysed solution was centrifuged  
197 at 12000 rpm, for 5 min at 4 °C to remove cell debris. The efficiency of cellular uptake in  
198 terms of the Fluorescence intensity of Rhodamine in the supernatant solution was measured  
199 using a FP-750 Spectrofluorometer (JASCO, Tokyo, Japan) at the excitation and emission  
200 range (550-590 nm).

201

202 *2.6. Qualitative cellular uptake analysis Apt-PEG-LPs in mTECs by confocal laser scanning*  
203 *microscopy (CLSM)*

204 For performing Confocal microscopy,  $2 \times 10^5$  mTECs were seeded per 35-mm glass  
205 bottom dish (Iwaki, Chiba, Japan) in 2 mL of culture medium 24 h before the experiment in a  
206 37 °C incubator under an atmosphere of 5% CO<sub>2</sub>, and in 95% humidity. On the next  
207 experimental day, the medium was removed from the cells by aspiration and the cells were  
208 then washed once with 2 mL of 1× PBS, and then incubated with 5 mole% of the total lipid of  
209 PEG-LPs, or Apt-PEG-LPs in Kreb's buffer for 3 h at 37 °C. After 2.5 h of incubation, 20 µl  
210 of Hoechst 33342 (1 mg/mL) was added to stain the nuclei and the suspension was re-  
211 incubated for an additional 30 min. The medium was then removed and the cells were washed  
212 twice with a 1 mL of 1× PBS supplemented with cholic acid (10 nM). Finally, 1 mL of Krebs  
213 buffer was added and the cells were analyzed under confocal microscopy (A1 Confocal Laser  
214 Microscope System, Olympus Instruments Inc., Tokyo, Japan).

215

216 *2.7. Intracellular trafficking of Apt-PEG-LPs in mTECs via Confocal laser scanning*  
217 *Microscopy (CLSM)*

218 mTECs were seeded in 35 mm glass bottom dish with 2 mL of medium and incubated for  
219 24 h. The cell density was  $2 \times 10^5$  cells /glass bottom dish. On the next experimental day, the  
220 cells were incubated with 5 mole% of the total lipid of Apt-PEG-LPs and PEG-LPs in Krebs  
221 buffer for 3 h at 37 °C under an atmosphere with 5% CO<sub>2</sub> and in 95% humidity. The cells  
222 were stained with LysoTracker green (DND-26) 1 (µg/ mL) for 30 min at 37 °C. After 2-3  
223 washings with 1× PBS supplemented with 10 nM cholic acid, the cells were examined by  
224 confocal laser scanning microscopy, as described above.

225

226 2.8. *Effect of uptake in competition of labeled Apt-PEG-LPs with excess unlabeled Apt-PEG-*  
227 *LPs*

228 Initially to confirm the pathway of aptamer modified PEGylated liposomes, a competition  
229 uptake assay was performed within labeled and unlabeled Apt-PEG-LPs in 1:2 molar ratios in  
230 mTECs. A total  $2 \times 10^5$  mTECs/glass bottom dish was prepared in the same manner as  
231 described above. Labeled and unlabeled Apt-PEG-LPs in Krebs buffer were subject to  
232 incubate in incubator with 3 h at 37 °C under an atmosphere with 5% CO<sub>2</sub> and in 95%  
233 humidity. After 2-3 washings with 1× PBS supplemented with 10 nM cholic acid, the cells  
234 were examined by confocal laser scanning microscopy, as described above.

235

236 2.9. *Investigation of the cellular uptake mechanism using excess unlabeled Apt-PEG-LPs by*  
237 *Confocal Laser scanning Microscope (CLSM)*

238 For the investigation of uptake mechanism, mTECs were prepared as described above.  
239 The cells were incubated with labeled and labeled-unlabeled (1:2 ratio) Apt-PEG-LPs (5  
240 mole% of the total lipid) in Kreb's buffer for 3 h at 37 °C under an atmosphere with 5% CO<sub>2</sub>  
241 and in 95% humidity. Apt-PEG-LPs were labeled with 1 μL Rhodamine (1 mM). After 2.5 h  
242 of incubation, 20 μl of Hoechst 33342 (1 mg/mL) was added to stain the nuclei and the  
243 suspension was re-incubated for an additional 30 min. After two to three washings, the cells  
244 in Krebs buffer were immediately subjected to analysis by confocal laser scanning  
245 microscopy.

246

247 2.10. *Qualitative and quantitative Evaluation of the different receptor mediated endocytic*  
248 *cellular uptake pathway*

249 For the qualitative CLSM studies to investigate the mechanism of internalization of the  
250 modified Apt-PEG-LPs,  $2 \times 10^5$  cells were seeded in a 35 mm glass bottom dish in 2 mL

251 medium and then incubated overnight at 37 °C in an atmosphere of 5% CO<sub>2</sub> and 95%  
252 humidity. The cells were washed with 1 mL of 1× PBS and then pre-incubated with Krebs's  
253 buffer for various times in the absence or presence of the following inhibitors: Amiloride (1  
254 mM) for 10 min; Sucrose (0.25 M) for 30 min or Filipin III (1 µg/mL) for 30 min at 37 °C.  
255 The various inhibitors were removed by aspiration, followed by washing once with Krebs  
256 buffer and the Apt- PEG-LPs were added to the cells, followed by incubation for 1 h at 37 °C.  
257 The cells were washed twice by adding 1 mL of PBS supplemented with 100 nM cholic acid.  
258 Finally the cells in 1 mL Krebs buffer were observed under the Confocal Laser scanning  
259 Microscope.

260 To quantitatively investigate the mechanism of internalization of the modified Apt-PEG-  
261 LPs,  $4 \times 10^4$  cells were seeded in a 24-well plate (Corning incorporated, Corning, NY, USA)  
262 and the plate was incubated overnight at 37 °C in an atmosphere of 5% CO<sub>2</sub> and 95%  
263 humidity. The cells were washed with 1 mL of PBS and then pre-incubated with Krebs's  
264 buffer for various times in the absence or presence of the following inhibitors: Amiloride (1  
265 mM) for 10 min; Sucrose (0.25 M) for 30 min or Filipin III (1 µg/mL) for 30 min at 37 °C.  
266 The various inhibitors were removed by aspiration, followed by washing once with Krebs  
267 buffer and then Apt- PEG-LPs were added in the cells to incubate for 1 h at 37 °C. The cells  
268 were washed twice by adding 1 mL of PBS supplemented with 100 nM cholic acid. Apt-  
269 PEG-LPs were added and the cells were incubated for 1 h at 37 °C. The cells were washed  
270 twice by adding 1 mL of PBS supplemented 100 nM cholic acid and the cells lysed with 1×  
271 Reporter lysss buffer at -80 °C for 20 min, and, after waiting for more than 20 min on the ice  
272 to melt the different liposomes solution, the treated cell suspensions were placed in 24-well  
273 plates. Finally the lysed solutions were centrifuged at 12000 rpm, for 5 min at 4 °C to remove  
274 cell debris. The efficiency of cellular uptake in terms of the Fluorescence intensity of  
275 Rhodamine in the supernatant solution was measured as described above.

276

277 *2.11. Qualitative Evaluation of the in vivo intratumoral localization of systemically injected*  
278 *Apt-PEG-LPs.*

279 Human renal cell carcinoma,  $1 \times 10^6$  OS-RC-2 cells, were subcutaneously injected on the  
280 right flank of mice. When the tumor volume reached  $100 \text{ mm}^3$ , the tumor-bearing mice were  
281 used for *in vivo* evaluation. Regarding the LPs, PEG<sub>5000</sub>-DSPE was incorporated to  
282 circumvent the clearance of LPs via the liver and spleen. Bare LPs were prepared as  
283 described above, and PEG<sub>5000</sub>-DSPE was then post-inserted by incubating the LPs with  
284 PEG<sub>5000</sub> and the Apt-PEG at 60 °C for 30 min (Apt/PEG<sub>5000</sub>-LPs). For the CLSM study, the  
285 fluorescent dye, DiI was administered at 1.0 mole% of the total lipid, and was added to the  
286 tubes when lipid film was prepared. Tumor-bearing mice was administered via the tail vein  
287 with the LPs at 750 nmol of lipid, and the tumor was then excised under anesthesia 6 h after  
288 the injection. To visualize the tumor vessels, FITC-isolectin B4 (Vector Laboratories,  
289 Burlingame, CA) was systemically injected into the tumor-bearing mice 10 min before the  
290 sample collection. The excised tumor tissue was observed by CLSM (Nikon A1, Nikon  
291 Instruments Inc., Tokyo, Japan). The total number of pixel of interest in each confocal image  
292 was calculated using the ImagePro-plus software (Media Cybernetics Inc., Bethesda, MD).  
293 Co-localization ratio with TECs was calculated according to the following equation; *Co-*  
294 *localization ratio with TECs = (yellow pixel) / (red pixel + yellow pixel)*. The above  
295 mentioned procedures were approved by the Hokkaido University Animal Care Committee in  
296 accordance with the Guidelines for the Care and Use of Laboratory Animals.

297

### 298 **3. Results**

299 *3.1. Synthesis of DNA aptamer AraHH001 conjugate with Maleimide-PEG<sub>2000</sub>-DSPE.*

300 Apt-PEG<sub>2000</sub>-DSPE was successfully synthesized by the conjugation of a 5-thiol-modified  
301 aptamer and 5 equimolar amounts of Maleimide-PEG-DSPE<sub>2000</sub>. MALDI-TOF mass was  
302 employed to confirm the conjugation (Fig. 1). Excess free lipid was successfully removed by  
303 overnight dialysis using 3500-5000 MWCO. The final quantification of Apt- PEG<sub>2000</sub>-DSPE  
304 was done by UV-Visible spectroscopy at 260 nm and the conjugation was ready for preparing  
305 liposomes.

306

### 307 3.2 Quantitative cellular uptake analysis of aptamer-modified PEG liposomes on mTECs by 308 spectrofluorometer

309 To demonstrate the function of our developed aptamer modified PEGylated Nanocarrier  
310 system that targeted primary cultured tumor endothelial cells, we first carried out an *in vitro*  
311 quantitative cellular uptake experiment using Rhodamine labeled 5mole% of the total lipid  
312 of PEG-LPs and Apt-PEG-LPs on mTECs. The relative fluorescence intensity of Apt-PEG-  
313 LPs was found to be almost 3.8 fold higher than that for PEG-LPs used as the control (Fig.  
314 2). The enhanced cellular uptake in terms of relative fluorescence intensity was statistically  
315 significant compared to control PEG-LPs.

316

### 317 3.3 Qualitative cellular uptake study of aptamer-modified PEG liposomes on mTECs by 318 CLSM

319 The cellular uptake of Apt-PEG-LPs and PEG LPs by mTECs was also tested by CLSM,  
320 as shown in (Fig. 3). The cellular uptake of PEG-LP was used as a negative control, showing  
321 a very weak fluorescence signal, representing that the only small amount of PEG-LPs were  
322 internalized into the cells. Compared to the control, our aptamer AraHH001 modified  
323 PEGylated liposomal nano-carrier system resulted in a higher uptake capacity, and at the

324 same time, showed an enhanced ability to recognize the target protein on cell surface  
325 receptors.

326

### 327 *3.4. Intracellular trafficking of aptamer modified PEGylated liposomes in mTECs by CLSM*

328 To demonstrate the actual localization of internalized aptamer modified PEGylated  
329 liposomes and or, either intact or particles that had escaped from endosomes and, or,  
330 underwent endosomal degradation, Rhodamine labeled Apt-PEG-LPs and PEG-LPs were  
331 incubated for 3 h with mTECs. The mTECs were stained with green lysotracker. A CLSM  
332 study showed that a certain portion of the Apt-PEG-LPs were merged with lysotracker,  
333 indicating that they were located in the lysosomal compartment (Fig. 4A). The remaining  
334 portions about 39% appeared as a non-colocalized form into the cells (Fig. 4B). Image Pro  
335 software (Media Cybernetics Inc., Bethesda, MD) was applied to count the pixels  
336 corresponding to the colocalized and noncolocalized area of Apt-PEG-LPs and PEG-LPs  
337 inside the cells.

338

### 339 *3.5. Competition with excess unlabeled Apt-PEG-LPs reduced the uptake of Apt-PEG-LPs*

340 To confirm the pathway responsible for the receptor mediated uptake of the Apt-PEG-LPs,  
341 we carried out a competition uptake assay with Rhodamine labeled and unlabeled (1:2) Apt-  
342 PEG-LPs in mTECs. Only Rhodamine labeled Apt-PEG-LPs was used in this uptake assay as  
343 a control (Fig. 5). The competition assay was successful in blocking the target receptor to a  
344 certain extent so that uptake inhibition was apparent compared to the control labeled Apt-  
345 PEG-LPs.

346

### 347 *3.6. Qualitative and quantitative uptake inhibition assay of Apt-mediated liposomes by* 348 *different endocytic inhibitors*

349 The entry route of cellular uptake of aptamer modified PEGylated liposomes was  
350 further examined by the presence of different endocytic pathway inhibitors. Different  
351 inhibitors such as Amiloride for macropinocytosis, sucrose for clathrin- mediated, Filipin for  
352 caveolae-mediated inhibitors [38] were used to determine the uptake rate for Apt-PEG-LPs.  
353 An *in vitro* CLSM uptake study in the presence of different inhibitors showed that the  
354 targeted Apt-PEG-LPs were inhibited significantly by clathrin mediated pathways,  
355 irrespective of whether other inhibitors had any influence on the uptake process (Fig. 6A). To  
356 further verify this conclusion, a quantitative analysis of uptake inhibition using different  
357 inhibitors was performed, as described above. The results indicated that the entry route  
358 followed by Apt-PEG-LPs was the same and the uptake was largely inhibited by sucrose (Fig.  
359 6B).

360

### 361 3.7. *In vivo* targeting ability of AraHH001 modified liposomes by CLSM observation

362 Finally, we investigated the *in vivo* targeting ability of the Apt-PEG-LPs. We speculated  
363 that the nucleic acid moiety of the Apt-PEG<sub>2000</sub>-DSPE might be recognized by immune cells  
364 due to the presence of negatively charged phosphodiester groups, and would consequently  
365 be excreted from the liver and spleen in which immune cells including macrophages and  
366 lymphocytes would also be excreted. To circumvent such non-specific clearance, the Apt-  
367 PEG-LPs were modified with PEG<sub>5000</sub>-DSPE (Apt/PEG<sub>5000</sub>-LPs). Fluorescence labeled-  
368 Apt/PEG<sub>5000</sub>-LPs were systemically injected into the human renal cell carcinoma (OS-RC-2  
369 cells) bearing mice, and the tumor tissue was then observed by whole mounting CLSM 6 h  
370 after the administration. We previously reported that free AraHH001 binds to TECs derived  
371 from OS-RC-2 cells [37]. As the Apt-PEG<sub>2000</sub>-DSPE was increased, the extent of co-  
372 localization of the LPs with tumor vessels was increased. When 5 mole% Apt-PEG-DSPE  
373 was incorporated, almost all of the LPs were observed in tumor vessels (Fig. 7). On the other

374 hand, LPs modified with 1 or 2.5 mole% Apt-PEG<sub>2000</sub>-DSPE were spread within the tumor  
375 xenograft. As to normal organs, the Apt-PEG-LPs were highly accumulated in the liver and  
376 spleen, but not in the heart, in which the target protein of AraHH001, troponin T, is expressed  
377 (Fig. S1).

378 To evaluate the selectivity of the Apt-PEG<sub>2000</sub>-DSPE modified LPs for the tumor  
379 vasculature, we next quantified the ratio of co-localization by pixel counting. The percentage  
380 of yellow pixels to the total number of red pixels was defined as a Co-localization ratio with  
381 TECs. The co-localization of the Apt/PEG<sub>5000</sub>-LPs with tumor vessels was compared with the  
382 Apt-LPs and only PEG-LPs. The PEG-LPs were accumulated in tumor tissue via the  
383 enhanced permeability and retention (EPR) effect [39], and then diffused from tumor vessels  
384 because PEG did not bind specifically to cancer cells and TECs. Representative images are  
385 shown in (Fig. S2). In fact, the PEG-LPs were found to be bound to TECs (3%), whereas  
386 the aptamer modified LPs were highly co-localized with the TECs (Apt-PEG-LPs 16%,  
387 Apt/PEG<sub>5000</sub>-LPs 25%) (Fig. 8).

388

#### 389 **4. Discussion**

390 Recently, our collaborative group isolated very pure tumor endothelial cells, in an attempt  
391 to better understand the effects of the tumor microenvironment on the properties of  
392 endothelial cells and showed they are different from normal endothelial cells. Additionally,  
393 tumor endothelial cells are cytogenetically abnormal. Thus, it can be assumed that cultured  
394 tumor endothelial cells are more relevant than normal endothelial cells in studies of tumor  
395 angiogenesis. It has been challenging to isolate and culture tumor endothelial cells because (i)  
396 endothelial cells are usually enmeshed in a complex type of tissue, consisting of vessel wall  
397 components, stromal cells, and tumor cells; and (ii) only a small fraction of cells within these  
398 tissues are endothelial cells. Our goal is Vascular targeting, an attractive strategy that takes

399 into account phenotype changes on the surface of endothelial cells under pathological  
400 conditions, such as angiogenesis and inflammation [32-36]. To achieve our goal, we first  
401 isolated a mTEC-specific DNA aptamer AraHH001 which confirms the selective expression  
402 not only on the surface of primary cultured mouse tumor endothelial cells of different origin,  
403 even it was expressed on the surface of primary cultured human tumor endothelial cells.  
404 Additionally, this isolated aptamer ligand has a tendency to be internalized by cells very well  
405 [37]. Therefore, our intent was to apply this promising, DNA aptamer ligand in the  
406 construction of an Apt-PEG-LPs nano-carrier system for further internalization studies to  
407 confirm its ability to target mTECs, thus leading to the development of a drug delivery  
408 system.

409 Both DNA and RNA aptamers for several different targets have been successfully screened in  
410 last two decades, and this approach is now considered to be the first choice probe and ligand  
411 for the development of future targeting nano-medicine [8-12]. We prepared an aptamer  
412 modified PEGylated nano-carrier system by attaching the 5- thioated aptamer ligand  
413 AraHH001 at the maleimide-PEG terminus on the liposomes. First, we cleave the  
414 AraHH001-S-S bond to produce an AraHH001-SH bond by treatment with a reducing agent  
415 TCEP. A NAP-column was used to purify the AraHH001-SH which was further used for the  
416 conjugation with maleimide-PEG<sub>2000</sub>-DSPE. Dialysis (MWCO 3500-5000) was performed  
417 until the pure aptamer-lipid conjugation was obtained. MALDI-TOF spectroscopy was  
418 employed to check the purity. Finally, the UV-visible spectroscopy was applied to measure  
419 the aptamer-lipid concentration. In this study, we attached our aptamer ligands to the distal  
420 ends of PEG chains. This would be more effective than directly attaching ligands to the  
421 surface of PEG-containing liposomes because, PEG chains interfere with both the coupling of  
422 ligands to the lipid bilayer and the interaction of these ligands with the intended biological

423 targets. These ligands coupled to the PEG terminus do not cause any interference with the  
424 binding of ligands to their respective recognition molecules [40].

425 First, we assessed an aptamer-decorated PEGylated nano-carrier system and found that is  
426 showed a significant level of cellular uptake compared to the unmodified PEGylated nano-  
427 carrier system in mTECs (Fig. 2). This result also indicated that the targeted aptamer first  
428 recognized the cellular surface of the target molecule and was then internalized. Next, to  
429 visualize the extent of enhanced cellular uptake we carried out an *in vitro* qualitative CLSM  
430 uptake study (Fig. 3). The Rhodamine labeled Apt-PEG-LPs were found to have a very  
431 higher internalization capacity in mTECs compared to unmodified PEG-LPs. Therefore, the  
432 above results suggest that modifying the PEGylated liposomes with the targeting ligand is  
433 essential for the association, and the internalization of the nano-carrier system into mTECs.  
434 At the same time, due to the steric repulsion of the PEG polymer to unmodified PEGylated  
435 Liposomes, the extent of association to the target mTECs is decreased, and thus the uptake  
436 efficacy was lower.

437 We next concentrated on a crucial step, i.e., addressing the distribution of ligand modified  
438 LPs, and their capacity to escape from endosomes. There is a very common but important  
439 phenomena called endosomal degradation that might interfere with the delivery of drugs or  
440 genes of a targeted carrier mediated nano-carrier to a specific site. To clarify this issue we  
441 carried out an intracellular trafficking experiment in which the uptake of Rhodamine labeled  
442 Apt-PEG-LPs was evaluated lysotracker green as an intracellular marker. A CLSM study of  
443 intracellular trafficking showed there some Apt-PEG-LPs were co-localized with lysotracker  
444 green as visualized as yellow (Fig. 4A). However, some remaining Apt-PEG-LPs that were  
445 un-colocalized but remained intact inside the cytoplasm could be observed (Fig. 4A).  
446 Whereas, PEG-LPs were not taken up substantially and therefore, it was difficult to  
447 determine whether they were colocalized or not. We then applied image pro software to count

448 different pixel areas and thus determine the co-localized, and non-co-localized areas of both  
449 the Apt-PEG-LPs and PEG-LPs. From the analysis of pixel counts it was found that the  
450 concentration of non-colocalized Apt-PEG-LPs was higher, than PEG-LPs. Next, we  
451 calculated the percent of non colocalized uptake for the Rhodamine signal of the Apt-PEG-  
452 LPs and PEG-LPs. Approximate 39% the Apt-PEG-LPs were non-colocalized, which was  
453 statistically significant as compared with the per sent uptake for the PEG-LPs (Fig. 4B).

454 We next explored the uptake mechanism responsible for the aptamer modified PEGylated  
455 nano-carrier system. Since we recently developed a DNA aptamer AraHH001 that  
456 specifically targets mTECs, it was applied in this project to develop a ligand based liposomal  
457 nano-carrier system. Our plan was to use unlabeled Apt-PEG-LPs to block the receptors  
458 (details can be found in the experimental section) from accessing the labeled Apt-PEG-LPs in  
459 a competition experiment. Only labeled Apt-PEG-LPs were used as a control to compare.  
460 The CLSM results suggested that, although not complete, that the inhibition of uptake of  
461 aptamer targeted nano-carrier occurred. This result, provides evidence to indicate that the  
462 uptake of Apt-PEG-LPs is a receptor mediated process (Fig. 5). We next investigated the  
463 specific pathway responsible for receptor mediated endocytosis, by using different receptor  
464 mediated endocytic inhibitors. The CLSM experimental results showed that our aptamer  
465 modified PEGylated nano-carrier system follows clathrin mediated endocytosis.

466 Receptor-mediated endocytosis is generally considered to be a very promising, and widely  
467 accepted approach to drug targeting. Most of the currently used ligands are internalized by  
468 clathrin-mediated endocytosis, consistent with our findings [38, 41]. Interestingly, our  
469 findings suggested that the newly developed aptamer ligand based PEGylated nano-carrier  
470 system exhibits a higher endosomal escaping capacity, although the exact reason for this is  
471 not currently clear. It is well known that poor intracellular trafficking is often associated with  
472 clathrin mediated endocytosis. Molecules entering a cell via this pathway rapidly experience

473 a drop in pH from neutral pH 5.9 to 6.0 in the lumen of early endosomes with a further  
474 reduction to pH 5 during progression from late endosomes to lysosomes, where ligands fused  
475 with it, eventually resulting in degradation [42]. However, it was previously reported that  
476 most ligands follow the clathrin mediated receptor specific endocytosis [43].

477 To date, only a few reports showing that aptamer modified liposomes are applicable to *in*  
478 *vivo* situations have appeared [24, 25]. To our knowledge, this is the first report to  
479 demonstrate the specific delivery of TECs using aptamer modified liposomes. The Apt-PEG-  
480 LPs and Apt/PEG<sub>5000</sub>-LPs were selectively bound to TECs, but not cancer cells after systemic  
481 injection. It is noteworthy that the PEG<sub>5000</sub>-DSPE modification appeared to facilitate the TEC  
482 delivery of Apt-PEG-LPs (Fig. 8). This can be attributed to the fact that the PEGylation  
483 partially covered the aptamers, and hence prevented them from being recognized by immune  
484 cells, such as macrophages. In previous reports, oligo nucleic acids were taken up via  
485 scavenger receptors [44], which are expressed in macrophages [45]. Accordingly, PEG<sub>5000</sub>-  
486 DSPE modification appears to improve the pharmacokinetics of Apt-PEG-LPs, and therefore  
487 Apt/PEG<sub>5000</sub>-LPs might be able to accumulate at much higher levels in tumor vessels than  
488 Apt-PEG-LPs.

489

## 490 **5. Conclusion**

491 We report on the development of an AraHH001 aptamer modified PEGylated liposomal  
492 nanocarrier system for targeted delivery toward tumor vasculature *in vitro* and *in vivo*. Our  
493 system enhanced specific cellular uptake in mTECs and has the capacity, to a certain extent,  
494 to escape from endosomes, a process that might be useful for future targeting drug delivery to  
495 tumor endothelial cells. We further confirmed that our Apt-PEG-LPs follow receptor specific  
496 and clathrin mediated endocytosis. Apt-PEG-LPs and Apt/PEG<sub>5000</sub>-LPs showed higher  
497 accumulation on tumor vasculature *in vivo*. The findings of our system complete all the

498 criteria that is primarily essential for a ligand based active drug delivery system, and would  
499 be very useful for the treatment of cancer and many related diseases.

500

### 501 **Acknowledgments**

502 This study was supported by grants from the Special Education and Research Expenses of the  
503 Ministry of Education, Culture, Sports, Science and Technology of Japan. This study was  
504 also supported by Grant-In-Aid for Young Scientists (B, 11018330) from the Ministry of  
505 Education, Culture, Sports, Science and Technology of Japan. The authors also thank Dr.  
506 Milton S. Feather for his advice in writing the English manuscript.

507

### 508 **References**

509

510 [1] Peer D, Karp JM, Hong S, Farokhzad OC, Margalit R, Langer R. Nanocarrier as an  
511 emerging platform for cancer therapy. *Nat Nanotechnol* 2007;2:751-760.

512 [2] Schrama D, Reisfeld RA, Becker JC. Antibody targeted drugs as cancer therapeutics. *Nat*  
513 *Rev Drug Discov* 2006;5:147-159.

514 [3] Gupta AK, Naregalkar RR, Vaidya VD, Gupta M. Recent advances on surface  
515 engineering of magnetic iron oxide nano-particles and their biomedical applications.  
516 *Nanomedicine* 2007;2:23-39.

517 [4] Zhang J, Yang PL, Gray NS. Targeting cancer with small molecule kinase inhibitors. *Nat*  
518 *Rev Cancer* 2009;9:28-39.

519 [5] Lammers T, Aime S, Hennink WE, Storm G, Kiessling F. *Acc Chem Res* 2011;44:1029-  
520 1038.

521 [6] Ellington AD, Szostak JW. *In vitro* selection of RNA molecules that bind specific ligands.  
522 *Nature* 1990;346:818-822.

- 523 [7] Tuerk C, Gold L. Systematic evolution of ligands by exponential enrichment, RNA  
524 ligands to bacteriophage T4 DNA polymerase. *Science* 1990;249:505-510.
- 525 [8] Shangguan D, Li Y, Tang Z, Cao ZC, Chen HW, Mallikaratchy P, *et al.* Aptamers  
526 evolved from live cells as effective molecular probes for cancer study. *Proc Natl Acad Sci*  
527 *USA* 2006;103:11838-11843.
- 528 [9] Morris KN, Jensen KB, Julin CM, Weil M, Gold L. High affinity ligands from in vitro  
529 selection, complex targets. *Proc Natl Acad Sci USA* 1998;95:2902-2907.
- 530 [10] Bunka DH, Stockley PG. Aptamers come of age – at last. *Nat Rev Microbiol*  
531 2006;4:588-596.
- 532 [11] Liss M, Petersen B, Wolf H, Prohaska E. An aptamer-based quartz crystal protein  
533 biosensor. *Anal Chem* 2002;74:4488-4495.
- 534 [12] Keefe AD, Pai S, Ellington A. Aptamers as therapeutics. *Nat Rev. Drug Discov*  
535 2010;9:537-550.
- 536 [13] Ruckman J, Green LS, Beeson J, Waugh S, Gillette WL, Henninger DD, *et al.* 2-  
537 Fluoropyrimidine RNA-based aptamers to the 165-amino acid form of vascular endothelial  
538 growth factor (VEGF 165). *J Biol Chem* 1998;273:20556-20567.
- 539 [14] Ni X, Castanares M, Mukherjee A, Lupoid SE. Nucleic acid aptamers: clinical  
540 applications and promising new horizons. *Curr Med Chem* 2011;18:4206-4214.
- 541 [15] Bangham AD, Standish MM, Watkins JC. Diffusion of univalent ions across the  
542 lamellae of swollen phospholipids. *J Mol Biol* 1965;13:238-252.
- 543 [16] Kaneda Y. Virosomes: evolution of the liposome as a targeted drug delivery system.  
544 *Adv Drug Deliv Rev* 2000; 43:197-205.
- 545 [17] Maurer N, Fenske D, Cullis PR. Developments in liposomal drug delivery systems.  
546 *Expert Opin Biol Ther* 2001;1:1-25.

547 [18] Torchilin VP. Recent advances with liposomes as pharmaceutical carriers. *Nat Rev Drug*  
548 *Discov* 2005;4:145-160.

549 [19] Immordino ML, Dosio F, Cattel L. Stealth liposomes: review of the basic science,  
550 rationale, and clinical applications, existing and potential. *Int J Nanomedicine* 2006;1:297-  
551 315.

552 [20] Willis MC, Collins B, Zhang T, Green LS, Sebesta DP, Bell C, et al. Liposome-anchored  
553 vascular endothelial growth factor aptamers. *Bioconjugate Chem* 1998;9:573-582.

554 [21] Cao Z, Tong R, Mishra A, Xu W, Wong GCL, Cheng J, et al. Reversible cell-specific  
555 drug delivery with aptamer-functionalized liposomes. *Angew Chem Int Ed* 2009;48:6494-  
556 6498.

557 [22] Kang H, O'Donoghue MB, Liu H, Tan W. A liposome-based nanostructure for aptamer  
558 directed delivery. *Chem Commun* 2010;46:249-251.

559 [23] Zhou J, Rossi JJ. Cell-specific aptamer-mediated targeted drug delivery.  
560 *Oligonucleotides* 2011;21:1-10.

561 [24] Xing H, Tang L, Yang X, Hwang K, Wang W, Yin Q, et al. Selective delivery of an  
562 anticancer drug with aptamer-functionalized liposomes to breast cancer cells in vitro and in  
563 vivo. *J Mater Chem B* 2013;1:5288-5297.

564 [25] Li L, Hou J, Liu X, Guo Y, Wu Y, Zhang L, et al. Nucleolin-targeting liposomes guided  
565 by aptamer AS1411 for the delivery of siRNA for the treatment of malignant melanomas.  
566 *Biomaterials* 2014;35:3840-3850.

567 [26] Hatakeyama H, Akita H, Harashima H. A multifunctional envelop type nano device  
568 (MEND) for gene delivery to tumours based on the EPR effect: a strategy for overcoming the  
569 PEG dilemma. *Adv Drug Deliv Rev* 2011;63:152-160.

570 [27] Folkman J. Tumor angiogenesis: therapeutic implications. *N Engl J Med*  
571 1971;285:1182-1186.

572 [28] Mehlen P, Puisieux A. Metastasis: a question of life or death. Nat Rev Cancer  
573 2006;6:449-458.

574 [29] Weigelt B, Peterse JL, van't Veer LJ. Breast cancer metastasis: markers and models. Nat  
575 Rev Cancer 2005;5:591-602.

576 [30] Folkman J. Angiogenesis: an organizing principle for drug discovery? Nat Rev Drug  
577 Discov. 2007;6:273-286.

578 [31] Ferrara N, Kerbel RS. Angiogenesis as therapeutic target. Nature 2005;438:967-974.

579 [32] Hida K, Klagsbrun M. A new perspective on tumor endothelial cells, unexpected  
580 chromosome and centrosome abnormalities. Cancer Res 2005;65:2507-2510.

581 [33] Hida K, Hida Y, Shindoh M. Understanding tumor endothelial cell abnormalities to  
582 develop ideal anti-angiogenic therapies. Cancer Sci 2008;99:459-466.

583 [34] Akino T, Hida K, Hida Y, Tsuchiya K, Freedman D, Muraki C, et al. Cytogenic  
584 abnormalities of tumor-associated endothelial cells in human malignant tumors. Am J Pathol  
585 2009;175:2657-2667.

586 [35] Matusda K, Ohga N, Hida Y, Muraki C, Tsuchiya K, Kurosu T, et al. Isolated tumor  
587 endothelial cells maintain the specific character during long-term culture. Biochem Biophys  
588 Res Commun 2010;394:947-954.

589 [36] Suzuki Y, Ohga N, Morishita Y, Hida K, Miyazono K, Watabe T. BMP-9 induces  
590 proliferation of multiple types of endothelial cells *in vitro* and *in vivo*. J Cell Sci  
591 2010;123:1684-1692.

592 [37] Ara MN, Hyodo M, Ohga N, Hida K, Harashima H. Development of a novel DNA  
593 aptamer ligand targeting to primary cultured tumor endothelial cells by a cell-based SELEX  
594 method. PLoS One 2012;7:e50174.

595 [38] Khalil IA, Kogure K, Akita H, Harashima H. Uptake pathways and subsequent  
596 intracellular trafficking in nonviral gene delivery. Pharmacol Rev 2006;58:32-45.

597 [39] Maeda H, Nakamura H, Fang J. The EPR effect for macromolecular drug delivery to  
598 solid tumors: Improvement of tumor uptake, lowering of systemic toxicity, and distinct tumor  
599 imaging *in vivo*. *Adv Drug Deliv Rev* 2013;65:71-79.

600 [40] Nallamouthu R, Wood GC, Pattillo CB, Scott RC, Kiani MF, Moore BM, et al. A tumor  
601 vasculature targeted liposome delivery system for combretastatin A4: design, characterization,  
602 and *in vitro* evaluation. *AAPS PharmSciTech* 2006;7:E32.

603 [41] Khalil IA, Kogure K, Futaki S, Harashima H. High density Octaarginine stimulates  
604 Macropinocytosis leading to efficient intracellular trafficking for gene expression. *J Biol*  
605 *Chem* 2006;281:3544-3551.

606 [42] Bally MB, Harvie P, Wong FM, Kong S, Wassan EK, Reimer DL. Biological barriers to  
607 cellular delivery of lipid-based DNA carriers. *Adv Drug Deliv Rev* 1999;38:291-315

608 [43] Lodish H, Berk A, Matsudaira P, Kaiser, CA, Krieger M, Scott MP, et al. *Molecular*  
609 *cell biology* 5th Ed. New York: WHFreeman; 2004:pp 618-655.

610 [44] Biessen EA, Vietsch H, Kuiper J, Bijsterbosch MK, Berkel TJ. Liver uptake of  
611 phosphodiester oligodeoxynucleotides is mediated by scavenger receptors. *Mol Pharmacol*  
612 1998;53:262-269

613 [45] Peiser L, Mukhopadhyay S, Gordon S, Scavenger receptors in innate immunity. *Curr*  
614 *Opin Immunol* 2002;14:123-128

615

616 **Figure legends**

617 Fig. 1. Conjugation of Apt-PEG<sub>2000</sub>-DSPE. (A). synthesis of thiol modified aptamer  
618 AraHH001 with maleimide-PEG<sub>2000</sub>-DSPE. Reduced aptamer and excess maleimide-  
619 PEG<sub>2000</sub>-DSPE were reacted in water overnight at 37 °C. (B). MALDI-TOF mass  
620 spectrometry was employed to confirm the conjugation.

621 Fig.2. Quantitative cellular uptake assay of Apt-PEG-LPs. SM-ECs, 4×10<sup>4</sup>/24-well were  
622 treated with 5 mole% of the total lipid of Apt-PEG-LPs or PEG-LPs for 3 h at 37 °C. The  
623 relative cellular uptake is expressed as mean ± SD. Statistical analysis of cellular uptake of  
624 Apt-PEG-LPs v's PEG-LPs was performed by unpaired student't test (n=5), \* P< 0.05,  
625 significant.

626 Fig.3. Qualitative CLSM cellular uptake assay of Apt-PEG-LPs. SM-ECs, 200000/35mm  
627 glass bottom dish were treated with 5 mole% of the total lipid of Apt-PEG-LPs or PEG-LPs  
628 for 3 h at 37 °C. PEG-LPs and Apt-PEG-LPs containing Rhodamine incubated with SM-ECs  
629 for 3 h at 37 °C. Nuclei were stained with Hoechst 33342.

630

631 Fig.4. Intracellular trafficking of Apt-PEG-LPs. (A) SM-ECs, 200000/35 mm glass bottom  
632 were treated with 5 mole% of the total lipid of Apt-PEG-LPs or PEG-LPs for 3 h at 37 °C.  
633 PEG-LPs and Apt-PEG-LPs containing Rhodamine incubated with SM-ECs for 3 h at 37 °C.  
634 Cells were stained with Green LysoTracker, and nuclei were stained with Hoechst 33342 for  
635 30 min. (B) Percent, % noncolocalize area of Apt-PEG-LPs. Image prosoftware were used  
636 to count the pixels corresponding to the Apt-PEG-LPs and unmodified PEG-LPs. Statistical  
637 analysis of different Apt-PEG-LPs v's PEG-LPs noncolocalized area was performed by  
638 unpaired student't test (n=5), \* P< 0.05, significant.

639

640 Fig.5. Competition of cellular uptake with excess unlabeled Apt-PEG-LPs. SM-ECs,  
641 200000/35 mm glass bottom dish was treated with labeled or labeled-unlabeled 5mol% of the  
642 total lipid of Apt-PEG-LPs for 3 h at 37 °C. Apt-PEG-LPs that contained Rhodamine, and  
643 nuclei were stained with Hoechst 33342 for 30 mins. (B) Percent, % noncolocalize area of  
644 Apt-PEG-LPs. Image prosoftware were used to count pixels of Apt-PEG-LPs and unmodified  
645 PEG-LPs. Statistical analysis of different Apt-PEG-LPs v's PEG-LPs noncolocalized area  
646 was performed by unpaired student't test (n=5), \* P< 0.05, significant.

647

648 Fig.6. Uptake inhibition assay of Apt-PEG-LPs by different inhibitors. Cells were pre-  
649 incubated in the absence or presence of 1 mM amiloride, 10 min, 1mg/mL Filipin, 30 min,  
650 0.25 M sucrose, 30 min SM-ECs, (A) In CLSM study, 200000 pre-incubated cells per 5 mm  
651 glass bottom were treated with 5 mole% of the total lipid of Apt-PEG-LPs for 1 h at 37 °C.  
652 Cells treated with only Apt-PEG-LPs used as a control. Apt-PEG-LPs containing Rhodamine,  
653 and nuclei were stained with Hoechst 33342 for 30 min (B) Quantitative inhibition of uptake  
654 of Apt-PEG-LPs were investigated using the above procedure. Here  $4 \times 10^4$  cells/24-well were  
655 used. After treatment  $1 \times$  lysis buffer (Promega) was used to lysate the cells. Finally, the  
656 quantification of fluorescent intensity was measured by spectrofluorometer. Data shown as  
657 mean  $\pm$  SD, n=4

658

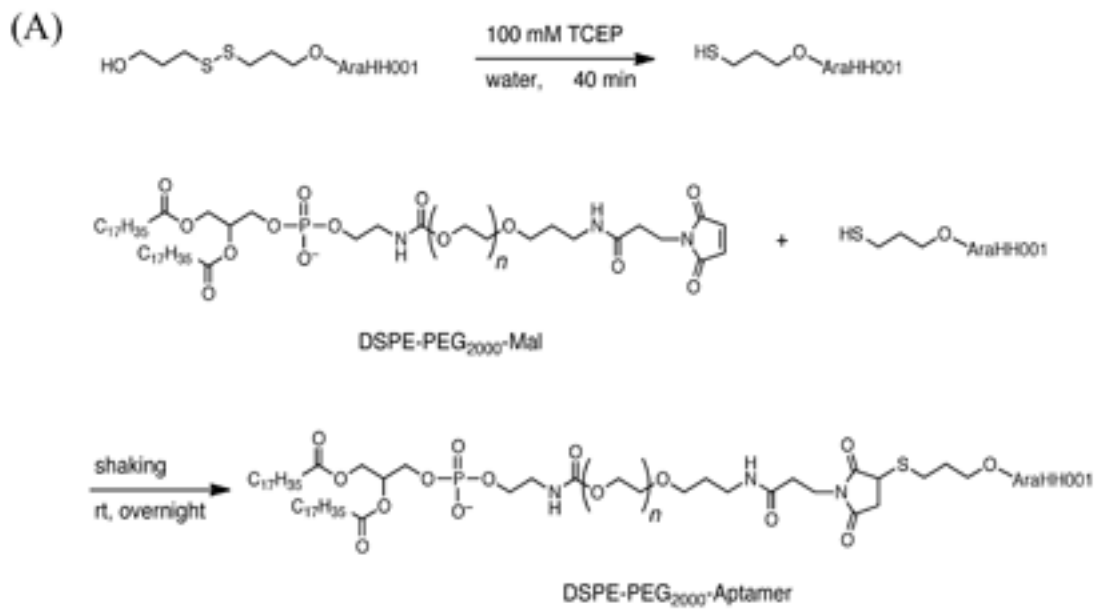
659 Fig.7. Intratumoral distribution of the Aptamer modified LPs. The fluorescently labeled-LPs  
660 were injected into the tumor-bearing mice at a lipid dose of 750 nmol, and tumor was  
661 collected 6 h after the injection. Prior to collection tumor vessels were visualized by FITC-  
662 labeled isoletin. Green and red dots indicate vessels and LPs, respectively.

663

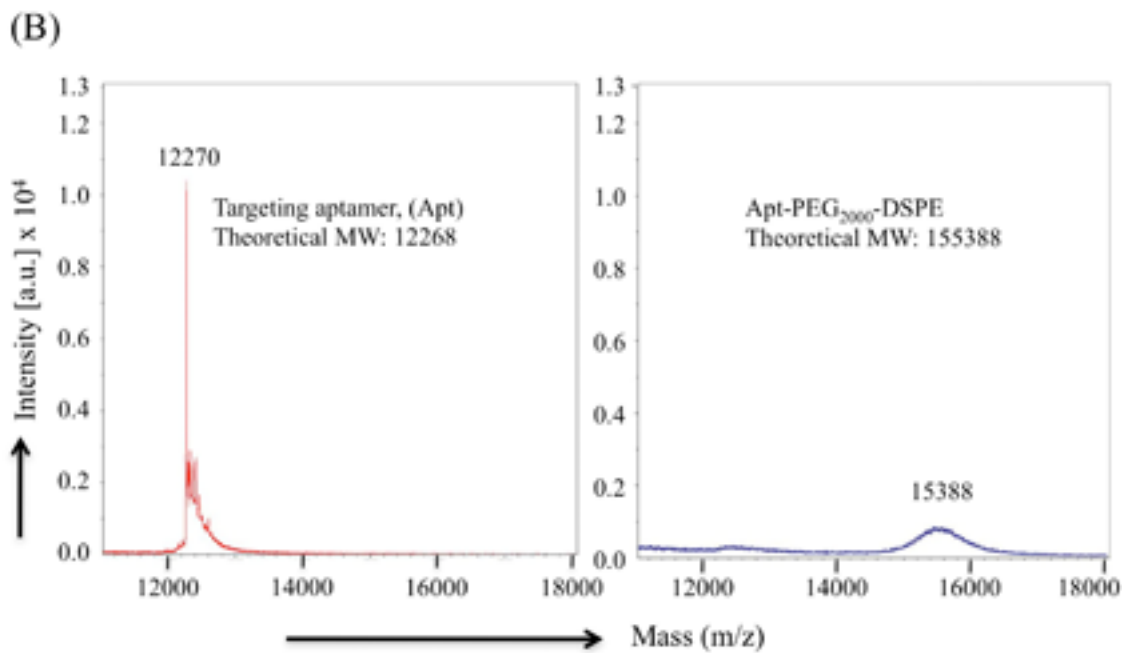
664 Fig.8. Investigation of the targeting efficiency to tumor vessels of the aptamer-modified LPs.  
665 Co-localization ratio with TECs were calculated by pixel counting the pictures (the  
666 representative images were indicated in Fig. S2) and calculating using the following  
667 equation; Co-localization ratio with TECs = (yellow pixels) / (red + yellow pixels). Data  
668 represents mean  $\pm$  SD. Statistical analysis was performed one way ANOVA followed by  
669 SNK test; \* P<0.05, \*\* P<0.01 v's PEG-LPs, n=3.

670

Fig. 1.



TCEP = tris(2-carboxyethyl)phosphine hydrochloride, efficient reducing agent for disulfide linkage



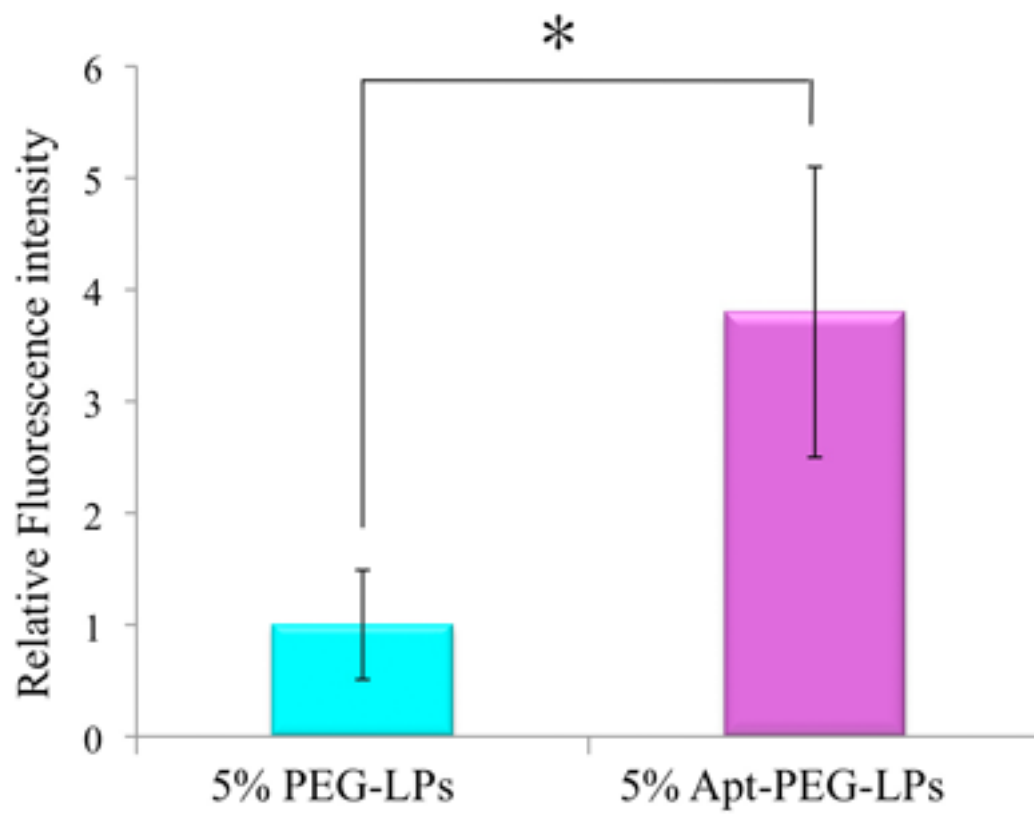
671

672

673

674

Fig. 2.

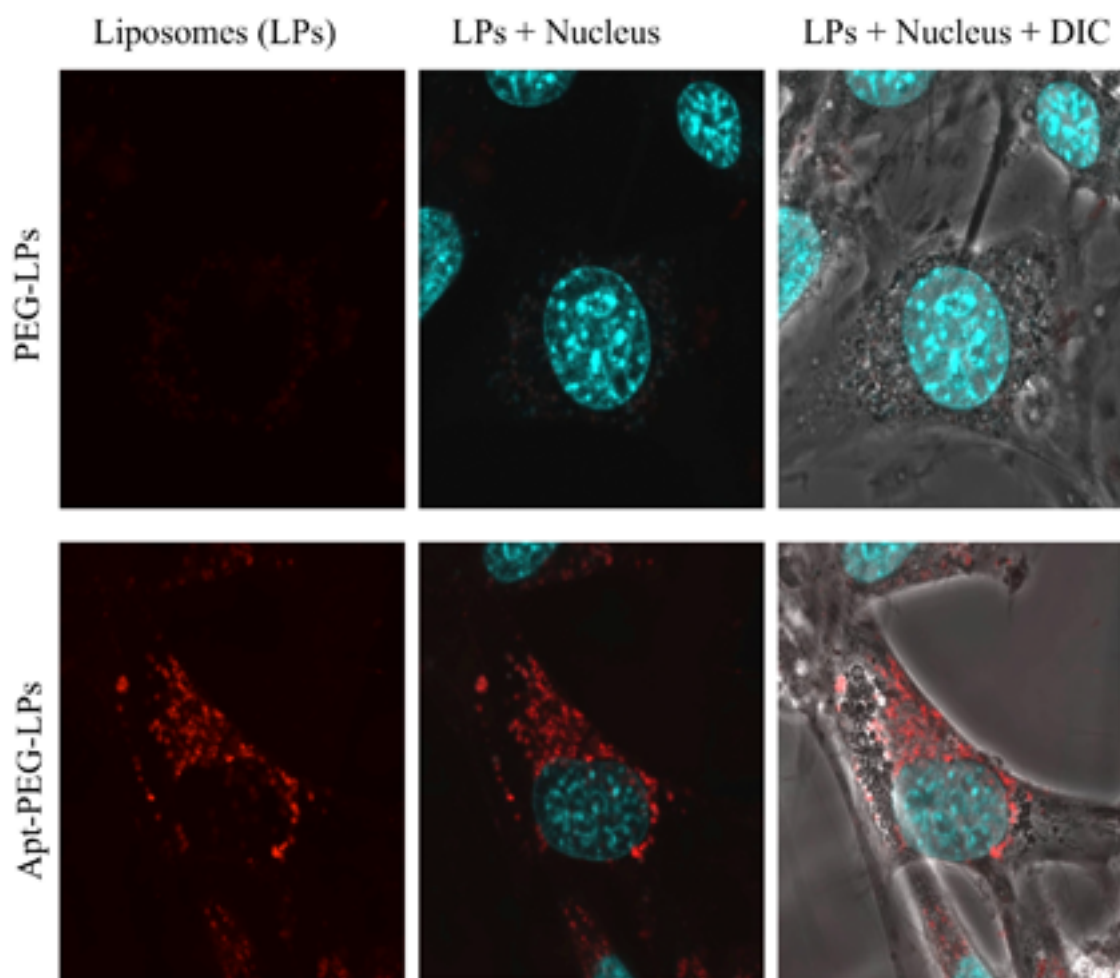


675

676

677

Fig. 3.

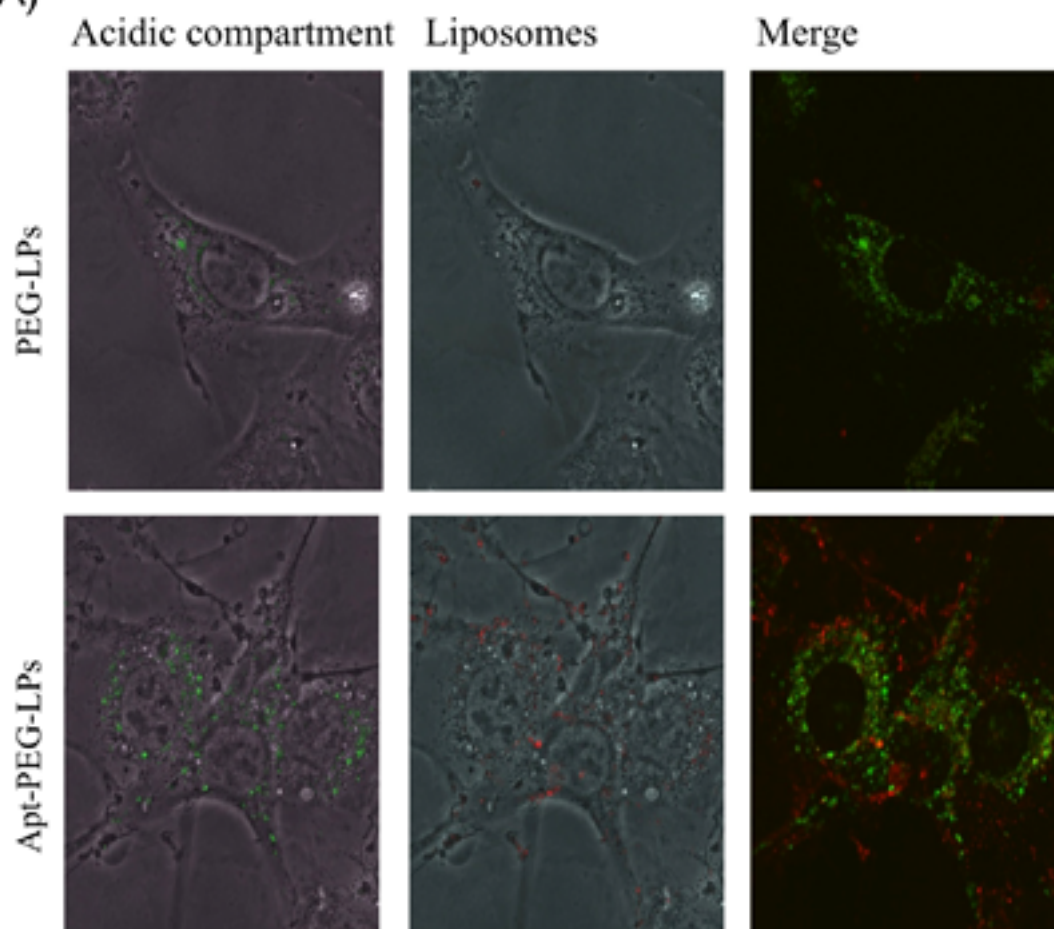


678

679

Fig. 4.

(A)



(B)

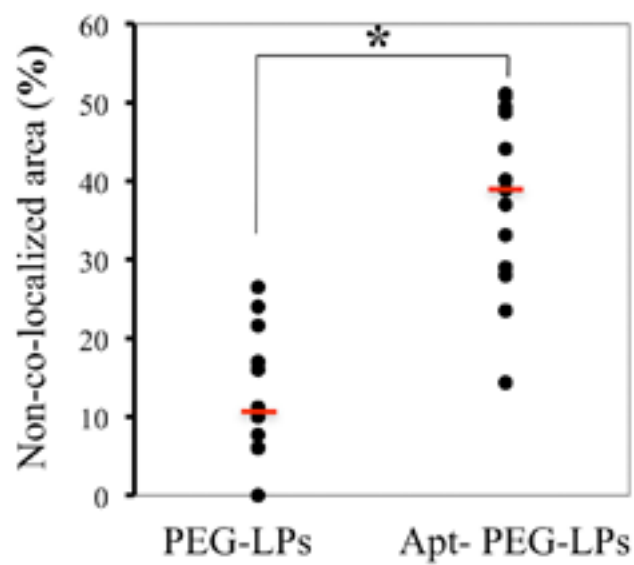
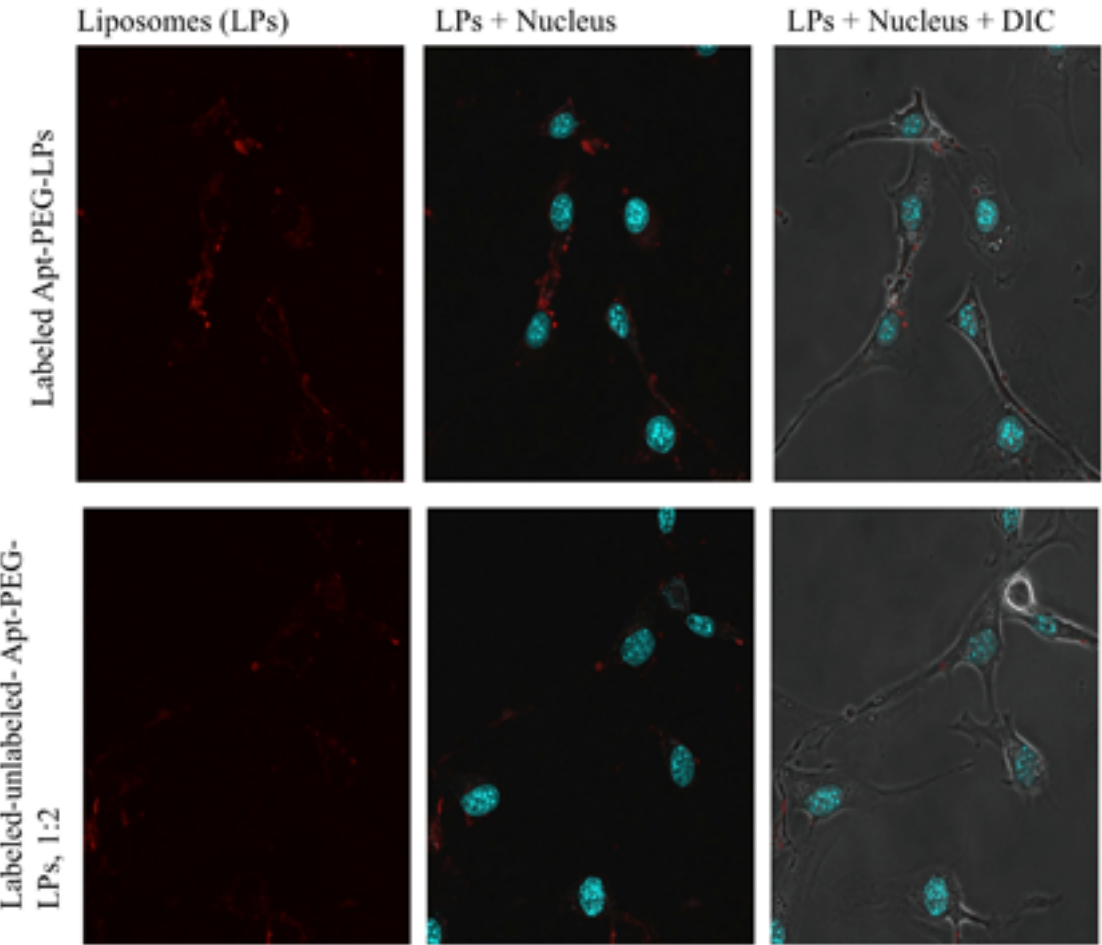


Fig. 5.

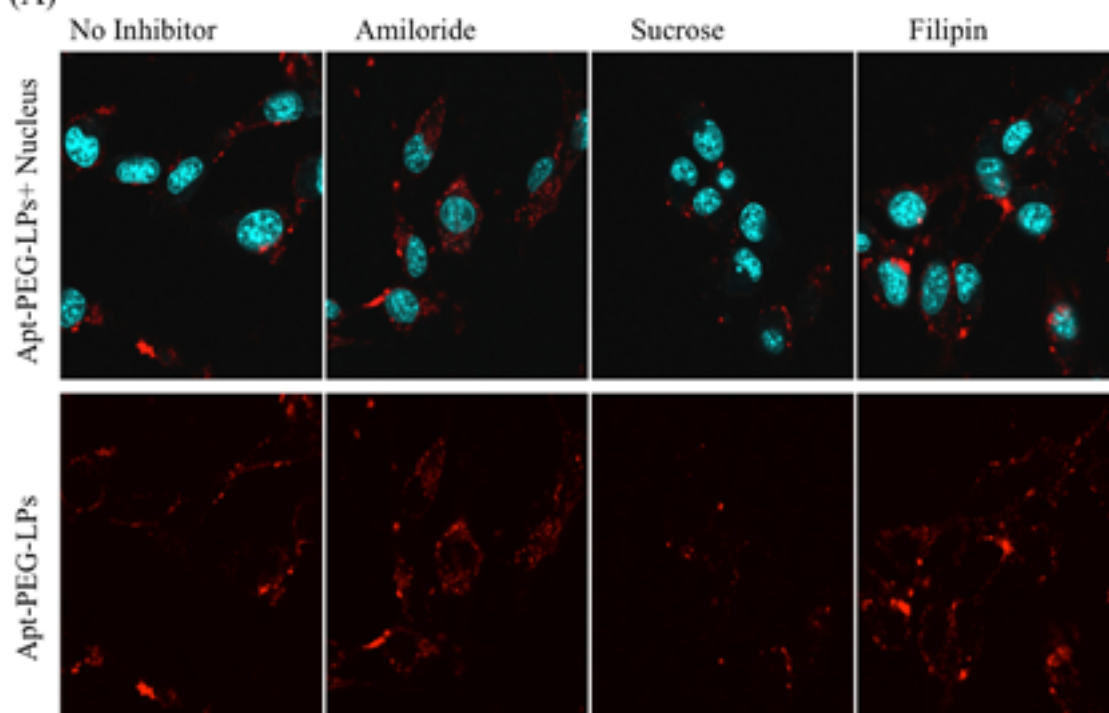


682

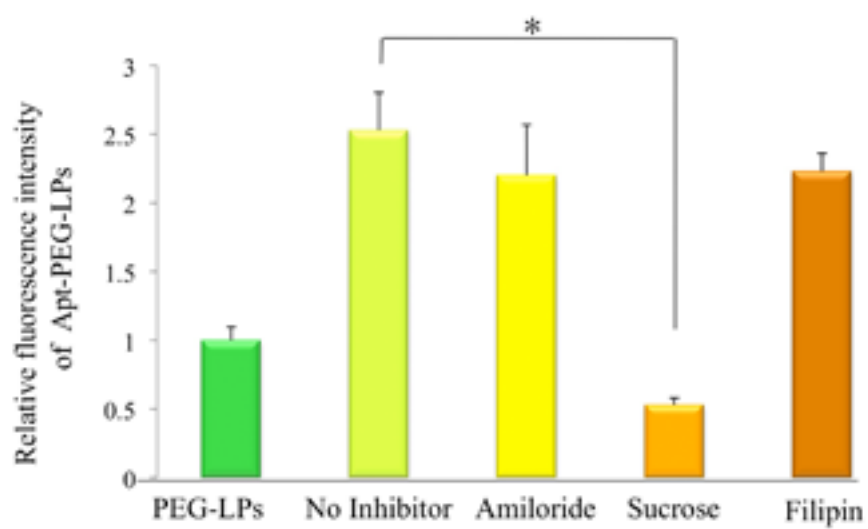
683

Fig. 6.

(A)



(B)

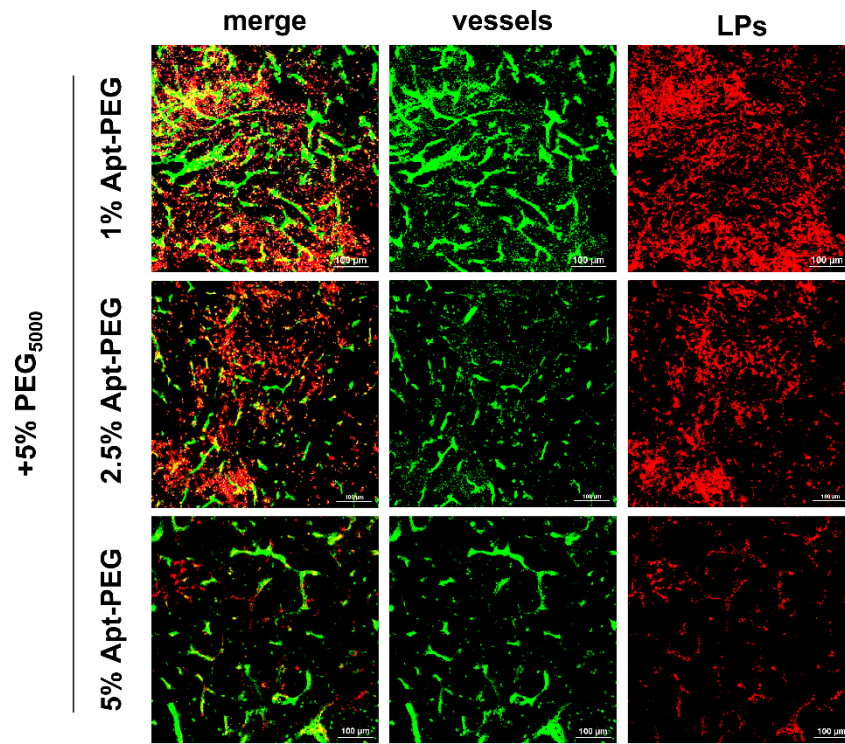


684

685

686

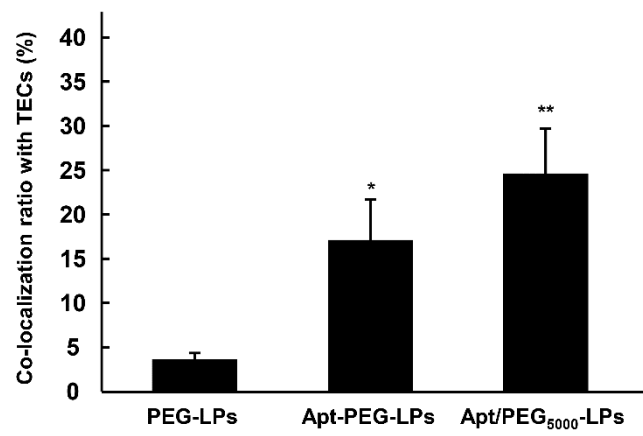
687 **Fig. 7**



688

689

690 **Fig. 8**



691